

# Numerical Simulation of the Effect of Evaporation of Liquid Droplets on Turbulence and Heat Transfer in a Droplet-Laden Flow behind a Backward-Facing Step

M. A. Pakhomov<sup>1\*</sup> and V. I. Terekhov<sup>1\*\*</sup>

<sup>1</sup>*Kutateladze Institute of Thermophysics, Siberian Branch, Russian Academy of Sciences, Novosibirsk, Russia*

Received April 5, 2022; in final form, August 10, 2022; accepted September 29, 2022

**Abstract**—The effect of evaporation of several types of liquid (water, ethanol, acetone, and glycerol) on the turbulence dynamics, propagation of the dispersed phase, and heat transfer in a backward-facing step for the droplet diameter  $d_1 = 1\text{--}100\ \mu\text{m}$  and mass fraction  $M_{L1} = 0\text{--}0.1$  was studied numerically. The two-fluid two-temperature Euler model was used for calculation of the motion and heat transfer in the droplet-laden flow. The system of Reynolds-averaged Navier–Stokes equations (RANS) written down with consideration of the presence and evaporation of droplets of different liquids was used in the work. The turbulent kinetic energy of the carrier gas phase was described using the model of transfer of the Reynolds stress model with consideration of the two phases of the flow. The effect of suppression of the turbulence of the carrier gas phase is minimal for acetone droplets (more than 7%) and maximal for glycerol and water droplets (up to 15%). The heat transfer enhancement at the use of ethanol droplets is maximal (more than two times compared with the single-phase separated flow), and evaporation of acetone droplets led to minimum heat transfer intensification (up to 25%).

**DOI:** 10.1134/S1810232822040051

## INTRODUCTION

Two-phase gas-droplet flows in various technical devices are usually anisotropic and can be complicated by the interfacial heat transfer, droplet evaporation, or flow separation. The two-phase flow behind a backward-facing step is one of the most common cases of shear flow around sharp edges of bodies [1–5]. The process is accompanied by significant changes in the velocity and pressure in the vicinity of the separation cross section. The presence of separation zone has a significant effect on the intensity of momentum and heat transfer processes and determines the structure of the turbulent flow. Sudden expansion of flow in flat ducts is commonly used as flame stabilizer in combustion chambers, for enhancement of heat and mass transfer processes, in various separators, and in many other technical devices.

Understanding of complex and multiscale processes of the motion and dispersion of evaporating droplets and their interaction with turbulent vortices in recirculation flows will enable more efficient use of two-phase flows in modern power equipment. However, to date, there is no detailed understanding of the aerodynamics and heat transfer even in the case of single-phase separated flow. One of important applications of separated two-phase flows is stabilization of combustion of evaporating fuel particles via creation of separation regions.

Among the studies of separated two-phase flows with solid particles after a backward-facing step (BFS) in the absence of interfacial heat transfer, we can note experimental [1–3] and numerical [4–9] works. The authors of these papers show that low-inertia particles are involved in the recirculation motion, whereas large particles do not get into the separation zone while passing through the shear flow region. They also note suppression of gas turbulence when small particles are added to the separated

\* Corresponding author. E-mail: [pakhomov@ngs.ru](mailto:pakhomov@ngs.ru)

\*\* E-mail: [terekhov@itp.nsc.ru](mailto:terekhov@itp.nsc.ru)

flow. To date, the literature offers few works on experimental [10, 11] and numerical [10, 13, 14] research on the flow structure, turbulence, and heat transfer in separated gas-droplet flows. Note that numerical calculations were carried out for the flow behind a sudden expansion of pipe [13] and for a gas-droplet flow behind a BFS. [14]. Experimental studies of two-phase gas-liquid flow of mixture of water and oil (petroleum) after a sudden expansion of the pipe were conducted in [15–17]. The authors constructed a map of two-phase flow regimes after the pipe expansion and presented the corresponding flow patterns.

The two-phase turbulent flow of gas and solid particles was studied in [18–20] with application of the large eddy simulation (LES) method for the gas phase and the Lagrangian trajectory method for the particles. In [21], a numerical simulation of turbulent gas-dispersed flow was carried out with the use of the lattice Boltzmann method (LBM). All the works were done for the isothermal case of flow behind a BFS [18, 19, 21] and behind a sudden expansion of the pipe [20]. The model in [19] does not take into account the reverse effect of the dispersed phase on the transfer processes and gas turbulence; the study was performed for the two-dimensional case of two-phase flow. In [18, 19, 21], a numerical simulation of flow behind a BFS was performed for the conditions of work [2]. It is shown that the accumulation of particles in the separation zone occurs at low Stokes numbers (small particle sizes). The results show that the dynamics of particle propagation in the separated flow strongly depends on the local level of turbulence of the carrier phase, especially so for small particles. However, large particles retain inertia along their trajectories, without reaction to gas pulsations. These conclusions qualitatively agree with those obtained for two-phase near-wall flows in ducts or pipes [22, 23].

The aim of this work is a numerical study of evaporation of droplets of various liquids (water, ethanol, acetone, and glycerol). These liquids differ markedly in the latent heats of evaporation and thermophysical properties. For instance, acetone and ethanol are volatile liquids, while glycerin does not evaporate at the temperature regime studied in the work.

This study is a continuation of our series of works [12–14, 24]. In the model in [12, 14, 24], we used our own numerical code to simulate a turbulent flow with droplets in a pipe with a sudden expansion. In a series of works [12, 14, 24], the Euler RANS model was developed and a numerical simulation of the flow and heat transfer during the evaporation of water droplets in a pipe with sudden expansion was performed. In [12, 14, 24], the turbulence of the carrier phase was calculated within the elliptic Reynolds stress model (second moment closure (SMC)) [25], the two phases of the flow taken into account [8]. All the above works of the group of authors were devoted to numerical study of the effect of evaporation of water droplets on the particle dynamics, modification of gas phase turbulence, and intensification of heat transfer in the separated flow.

## 1. MATHEMATICAL MODEL

### *1.1. Governing Equation Set for Turbulent Polydispersed Bubbly Flow*

For description of two-phase flow, two main calculation methods are offered: the Eulerian and Lagrangian ones [26, 27]. The first method, the Eulerian continuous description, employs the so-called two-fluid models. The second method applies the Lagrangian trajectory approach [27, 28]. Both methods have their pros and cons and complement each other, advantages of one approach being disadvantages of the other. For description of the dynamics of the dispersed phase in two-phase turbulent flows, including in the presence of a sudden expansion of the flow, both the Eulerian and Lagrangian approaches are used.

The paper considers the problem of dynamics of a turbulent gas-droplet separated flow in the presence of heat transfer with the channel wall. The solution uses two-dimensional RANS equations [12, 14, 24], written down with consideration of the effect of particles on the transport processes in the gas [8]. The use of the SMC approach makes it possible to abandon the hypothesis of isotropic viscosity, strictly speaking, inapplicable for calculating separated flows [29, 30]. For description of the dynamics of the flow and heat and mass transfer in the gaseous and dispersed phases, the Eulerian continuous approach or the so called two-fluid and two-temperature models is used [22, 23, 26, 27]. The problem of dynamics of a gas-droplet turbulent separated flow in the presence of heat transfer with the channel walls is considered. Figure 1 presents a schematic representation of the flow. The volume fraction of the dispersed phase is low ( $\Phi_1 = M_{L1}\rho/\rho_L < 10^{-4}$ ), and the particles are rather small ( $d_1 < 200 \mu\text{m}$ ). Therefore, the effects of their collisions with each other can be neglected [23, 23, 27]. Here  $M_{L1}$  is the initial mass concentration of the droplets and  $\rho$  and  $\rho_L$  is the density of the gas and droplets, respectively.

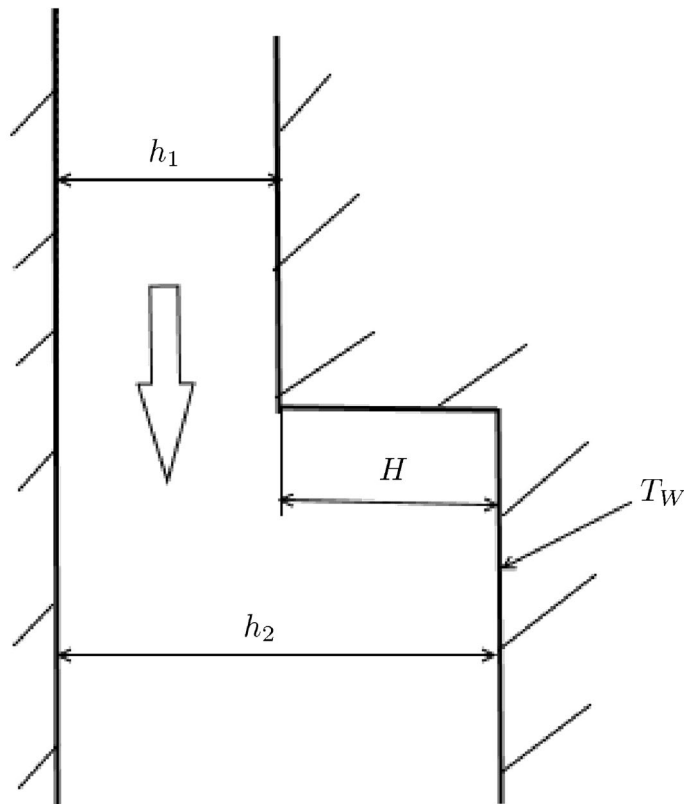


Fig. 1. Scheme of development of two-phase flow behind flat backward-facing step.

### 1.2. Numerical Realization

The numerical solution was found by the finite volume method on staggered meshes. For the convective terms of the differential equations, the QUICK procedure of the second order of accuracy was used. For the diffusion fluxes, central differences of the second order of accuracy were applied. The correction of the pressure field was performed according to the agreed finite volume procedure SIMPLEC. All calculations were done on the basic mesh of  $400 \times 100$  control volumes (CVs). The length of the calculated section after the expansion of the pipe was  $30H$ , where  $H$  is the step height. For verification of the independence of the solution on the number of computational cells, calculations were also carried out on meshes containing  $200 \times 50$  CVs ("coarse" mesh) and  $500 \times 150$  CVs ("fine" mesh). The difference in the calculation results for the basic and "fine" meshes is less than 0.1%. Further increase in the number of CVs does not significantly affect the results of numerical calculations. The calculations were performed on a mesh with thickening toward all solid surfaces, in the flow recirculation region. A coordinate transformation suitable for such a two-dimensional problem was used:  $\Delta\psi_j = K \times \Delta\psi_{j-1}$ , where  $\Delta\psi_j$  and  $\Delta\psi_{j-1}$  are the current and previous mesh steps in the axial or radial direction, and  $K = 1.08$  and  $1.06$  (in the longitudinal and transverse directions). At least 10 CVs were used for resolving of the mean flow field and turbulent characteristics of two-phase flow in a viscous sublayer ( $y_+ < 10$ ).

On the pipe axis, conditions for smooth conjugation for both phases are set. Boundary conditions from [31] are used for the dispersed phase on the channel wall. It is taken that after the contact with the bounding surface, the droplet evaporates instantly and becomes a source of vapor mass and a sink of heat necessary for its evaporation heating. In the exit section, conditions of zero derivatives of all the desired parameters in the longitudinal direction are set.

## 2. NUMERICAL RESULTS AND THEIR DISCUSSION

All numerical calculations were performed for a monodispersed mixture of air with droplets of various liquids at the inlet to the channel, for the case of downward motion of two-phase flow. Further, after the

cross section of the sudden separation of the flow, the droplet size decreases due to their evaporation, both in the longitudinal and transverse directions. The air duct height before the sudden expansion is  $h_1 = 20$  mm; after expansion it is  $h_2 = 40$  mm; the backward-facing step height is  $H = 20$  mm; the expansion ratio  $ER = h_2/h_1 = (h_1 + H)/h_1 = 2$  (see Fig. 1). The mass-average gas velocity in the flow detachment cross section varies,  $U_{m1} = 5\text{--}20$  m/s, and the Reynolds number for the gas phase, constructed from the mass-average gas velocity at the inlet and step height, is  $Re_H = HU_{m1}/\nu \approx (0.66\text{--}2.66) \times 10^4$ .

2.1. Flow Structure

Figures 2 and 3 display the profiles of the averaged longitudinal velocity and temperature of the gas phase in the single-phase (solid lines) and gas-droplet (dashed lines) flows, respectively, along the channel length in the wall units. The bold lines in Fig. 2 show the velocity profile in the wall coordinates for the single-phase stabilized flow in the channel, described by the following dependences [32]:

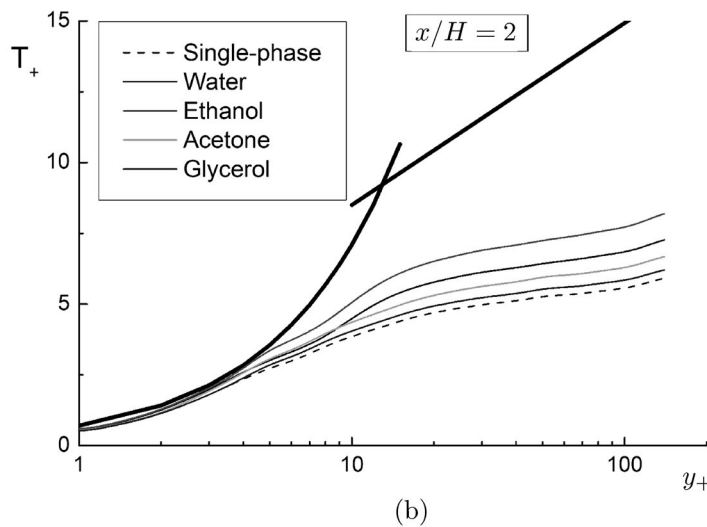
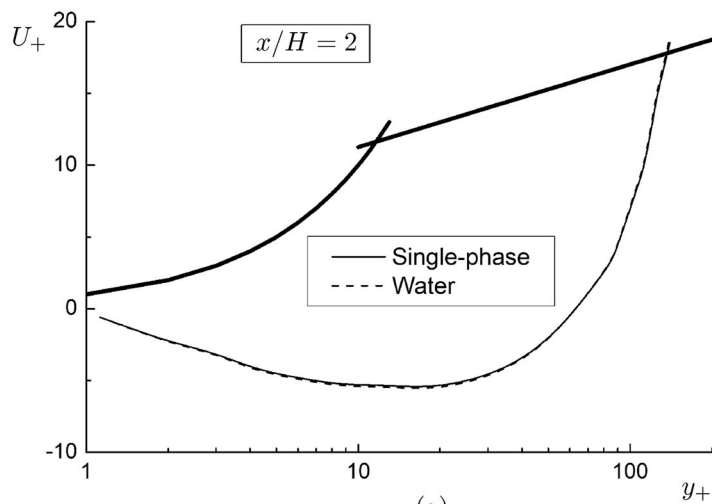


Fig. 2. Profiles of (a) averaged longitudinal velocity component and (b) gas phase temperature in universal logarithmic coordinates.  $M_{L1} = 0.05$ ,  $d_1 = 30 \mu\text{m}$ ,  $Re_H = 1.33 \times 10^4$ .

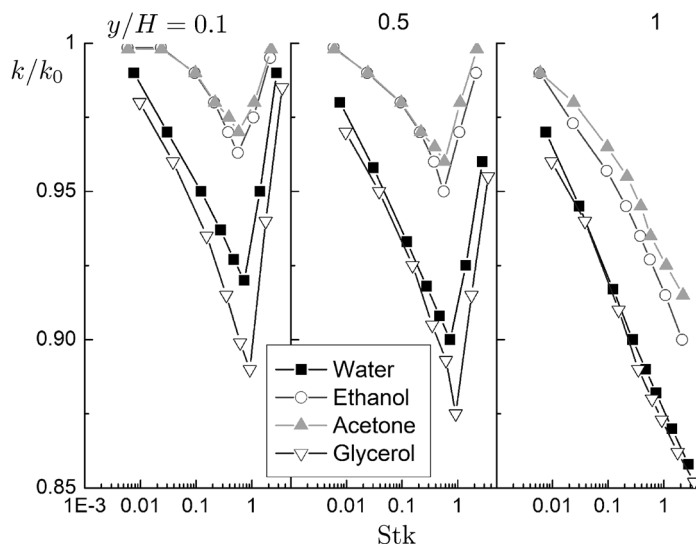


Fig. 3. Variation of turbulence modification parameter in gas-droplet flow behind backward-facing step.  $M_{L1} = 0.05$ ,  $x/H = 2$ ,  $Re_H = 1.33 \times 10^4$ .

$$\begin{cases} U_+ = y_+, \\ U_+ = 2.5 \ln y_+ + 5.5, \end{cases}$$

where  $U_+ = U/u_*$ ,  $u_* = (\tau_W/\rho_W)^{0.5}$  is the friction speed, and  $y_+ = yu_*/\nu$  is the dimensionless distance from the channel wall. The profiles were calculated versus the influence of the mass concentration of particles (a) and their initial size (b). For clarity, the velocity profiles in the wall coordinates are shown in Fig. 2 only for the two-phase flow with water droplets. For other liquids, the difference in the simulation results was insignificant as compared with water droplets.

The dimensionless temperature of the gas phase, written down in universal coordinates, was determined from the relation  $T_+ = (T_W - T_m)/T_*$ , where  $T_* = (\lambda/\rho C_p u_*) (\partial T/\partial y)_W$  is a thermal analogue of the friction velocity [33]. The bold lines in Fig. 3 show the temperature profile in the wall coordinates for the single-phase stabilized flow in the channel, described by the following dependencies [32]:

$$\begin{cases} T_+ = \text{Pr } y_+, \\ T_+ = 2.79 \ln y_+ + 2.08, \end{cases}$$

where  $\text{Pr} = 0.71$  is the molecular Prandtl number.

The results of numerical calculations of the average longitudinal velocity and temperature are below the classical logarithmic distributions. The profiles of the average longitudinal velocity (see Fig. 2) and temperature (see Fig. 3) written down in the wall units in the separated flow differ markedly from the classical logarithmic distributions for the flow in a channel [32]. This indicates a difference in the mechanisms of the momentum and heat transfer in two-phase misty separated flows compared with the classical single-phase turbulent boundary layer. For the velocity profiles, the effect of droplet evaporation on the velocity distributions is minor (see Fig. 2). However, for the gas temperature profiles, a noticeable difference is observed during the evaporation of various liquids (see Fig. 3). The temperature profiles of the gas phase in the two-phase flows are much higher than those for the single-phase flow. This indicates intensification of heat transfer during the evaporation of liquid droplets. The greatest differences were observed for evaporation of ethanol and water droplets, and the smallest differences were seen for droplets of glycerol (since it does not evaporate under these temperature conditions) and acetone. The velocity profiles in the region of separation of the two-phase flow ( $x/H < 7$ ) exhibit presence of negative

velocities (flow recirculation zones). The longitudinal velocity and temperature profiles tend to recovery to the fully developed flow regime in a plane channel at a large distance from the flow reattachment point ( $x/H = 15$ ).

Figure 3 shows variation of the turbulent kinetic energy (TKE) of the gas phase in the gas-droplet flow after a sudden expansion of the channel versus the mean-flow Stokes number  $Stk$ . Here  $k_0$  is the level of turbulence of the gas phase in the single-phase flow. The mean-flow Stokes number  $Stk = \tau/\tau_f$ , where  $\tau = \rho_L d^2/(18\mu W)$  is the particle relaxation time, written down with consideration of the deviation from the Stokes flow law,  $\tau_f = 5H/U_{m1}$  is the time scale of the carrier phase (passage frequency of large vortices) [2, 10],  $W = 1 + 0.15Re_L^{0.687}$ , and  $Re_L = |\mathbf{U}_S - \mathbf{U}_L|d/\nu$  is the Reynolds number for the dispersed phase, determined for the interfacial velocity. Here  $U_{S,i} = U_i + \langle u'_s \rangle_i$  is the actual gas velocity at the particle location point (gas velocity seen by the particle) and  $U_L$  is the average drop velocity, where  $U$  is the average gas velocity (obtained from the RANS calculation),  $\langle u'_s \rangle$  is the drift velocity between the liquid and particles [8], and  $\nu$  is the kinematic viscosity. The numerical simulation is carried out in the wide range of mean-flow Stokes numbers  $Stk = 0.01-3.5$ . With increase in the droplet diameter at the inlet, the suppression of the turbulence of the carrier phase grows. The least suppression of turbulence for all particle materials is observed in the near-wall part of the channel at  $y/H = 0.1$ , and the degree of turbulence gradually decreases as the distance from the heated channel wall grows. The maximum suppression of turbulence for all distances from the wall is obtained for glycerol droplets, and the smallest effect is seen for acetone and ethanol droplets. This is explained by the fact that droplets of acetone and ethanol evaporate intensely, while droplets of glycerol practically do not evaporate under these conditions and behave almost like solid particles. Evaporating water droplets exhibit intermediate suppression of the TKE level of the gas phase.

Figure 4 shows distributions of the mass concentration of droplets of various liquids versus the Stokes number. Here  $M_{L1}$  is the mass concentration of droplets in the inlet cross section. Obviously, due to the heat transfer with the heated channel wall, the droplet concentration is the lowest in the near-wall region  $y/H = 0.1$  and the highest far from the heated channel wall at  $y/H = 0.5-1$ . The lowest droplet concentrations are for acetone as the most easily evaporating liquid. The highest concentrations of the dispersed phase are for droplets of glycerol and water. The near-wall region of the channel ( $y/H = 0.1$ ) is practically free from small droplets (the Stokes number  $Stk < 0.1$ ,  $d_1 < 10 \mu m$ ) due to their fast heating and evaporation process, and here  $M_L/M_{L1} \approx 0$ . The only exception are glycerol droplets, which do not evaporate under the given temperature conditions, are present in the recirculation region of the flow, and affect the turbulence of the carrier phase (see Fig. 3). Increase in the droplet diameter (at a

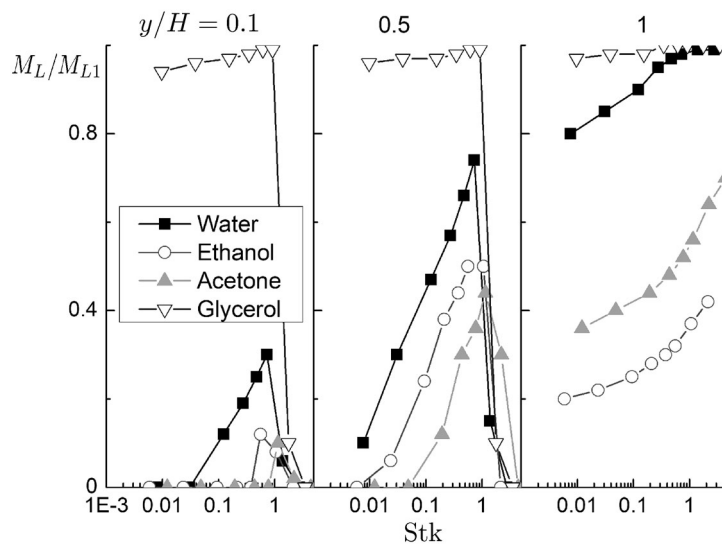


**Fig. 4.** Influence of mean-flow Stokes number on change in mass concentration of dispersed phase.  $M_{L1} = 0.05$ ,  $x/H = 2$ ,  $Re_H = 1.33 \times 10^4$ .

fixed concentration) leads to significant reduction of the interfacial surface. Therefore, further, as the droplet diameter (Stokes number) grows, the droplet concentration goes up because of their slower heating up and evaporation. This is what explains the presence of a local maximum in the concentration distributions for  $y/H = 0.1$  and  $0.5$ . Large particles at  $Stk > 1$  practically do not penetrate into this part of the channel (recirculation region) because of their weak involvement in the turbulent gas flow and, therefore, the  $M_L/M_{L1}$  value decreases sharply and  $M_L/M_{L1} \rightarrow 0$ . Evaporation of droplets in the flow core at  $y/H = 1$  is extremely minor, and the mass concentration profiles for all droplet diameters and types are almost constant.

## 2.2 Heat Transfer

Figure 5 show the influence of the mean-flow Stokes number (Fig. 5a) and the initial mass concentration of droplets (Fig. 5b) of various liquids on the magnitude of the maximum local and average heat transfer. The dashed lines in these figures display the data for the maximum heat transfer in the single-phase separated flow,  $Nu_{\max} \approx 61$  at  $M_{L1} = 0$ . Initially, in the region of small particle sizes ( $Stk \approx 0.1$ ), there is observed a slight noticeable growth of the heat transfer intensity with increase in the Stokes

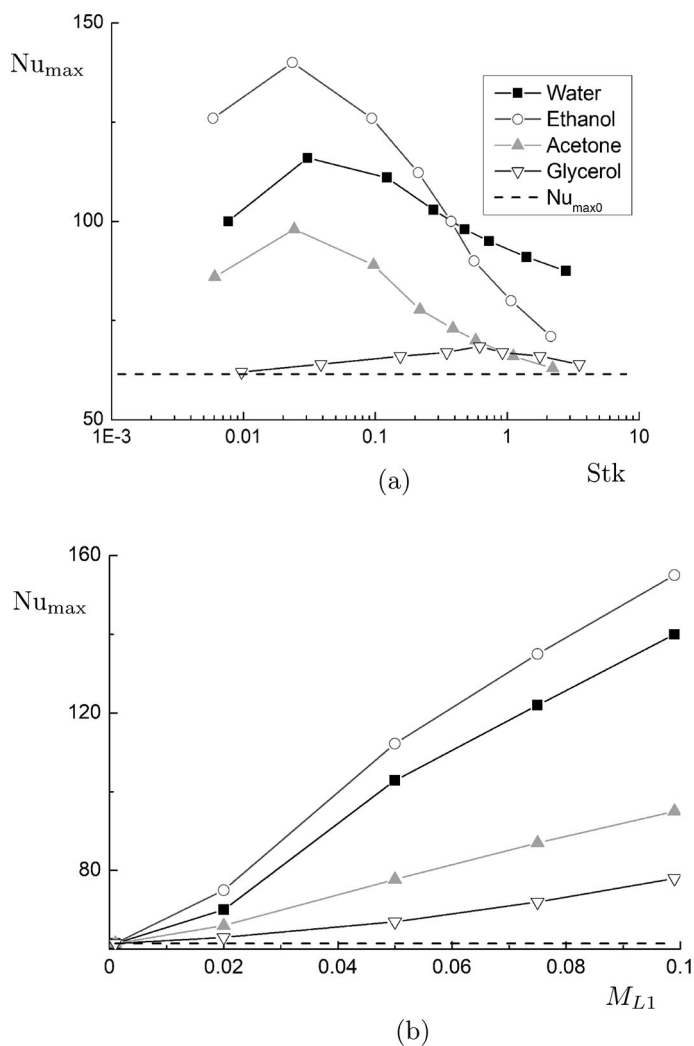


**Fig. 5.** Effect of (a) mean-flow Stokes number and (b) mass concentration of droplets of various liquids on distribution of maximum Nusselt number in two-phase separated flow behind backward-facing step. (a):  $M_{L1} = 0.05$ ; (b):  $d_1 = 30 \mu\text{m}$ .

number (initial droplet diameter), after which it sharply decreases. Such behavior of the maximum heat transfer value is due to the influence of factors of different nature: more intense evaporation of small-diameter droplets, decrease in the rate of their inertial deposition, and weakening of the involvement of large particles into the separated flow. Increase in the mass concentration of the dispersed phase causes significant heat transfer enhancement in the two-phase flow compared with the single-phase one (dashed line,  $M_{L1} = 0$ ). Note that the largest intensification of the heat transfer in the gas-droplet flow occurs in the region of small-size particles, which penetrate into the recirculation zone to the heated pipe wall and, evaporating in this region, enhance the heat transfer between the channel wall and the two-phase flow.

The greatest increase in the heat transfer intensity (up to 2.4 times compared with the single-phase flow) was obtained for evaporation of ethanol droplets, and the minimum increase (up to 1.6 times) was at evaporation of acetone droplets. For glycerin, which does not evaporate under these conditions, practically no heat transfer intensification is observed. It should be noted that water droplets evaporate more slowly due to the high value of the phase transition heat. The heat transfer enhancement does not exceed 2 times; due to the slower evaporation of droplets, the effect of heat transfer growth increases for the case of large droplet sizes. It is quite obvious that increase in the mass concentration of droplets at the inlet for all types of liquids enhance the heat transfer because of the larger number of droplets and, accordingly, the larger area of the interfacial surface.

## CONCLUSION

The effect of evaporation of a few types of liquid (water, ethanol, acetone, and glycerol) on the change in the turbulence, propagation of the dispersed phase, and heat transfer in a backward-facing step is numerically studied for the droplet diameters  $d_1 = 1\text{--}100\ \mu\text{m}$  and mass fraction  $M_{L1} = 0\text{--}0.1$ .

The RANS model developed earlier by the authors of the article in the Eulerian approximation was used to simulate the turbulent flow of gas with droplets of various liquids behind a backward-facing step. The turbulent kinetic energy of the carrier gas phase is described within the Reynolds stress model with consideration of the two phases of the flow. The effect of suppression of the turbulence of the carrier gas phase is minimal for acetone droplets (more than 7%), and is maximal for glycerol and water droplets (up to 15%). The heat transfer enhancement is maximal (more than 2 times compared with the single-phase separated flow) with the use of ethanol droplets and minimal at evaporation of acetone droplets (up to 25%).

## FUNDING

The numerical results were obtained with the financial support of the RF Ministry of Science and Higher Education (mega-grant 075-15-2021-575).

## REFERENCES

1. Ruck, B. and Makiola, B., Particle Dispersion in a Single-Sided Backward-Facing Step Flow, *Int. J. Multiphase Flow*, 1988, vol. 14, pp. 787–800.
2. Fessler, J.R. and Eaton, J.K. Turbulence Modification by Particles in a Backward-Facing Step Flow, *J. Fluid Mech.*, 1999, vol. 314, pp. 97–117.
3. McAndrew, D., Coppen, S., and Rogers, C.B., Measurements of Fluid Turbulence along the Path of a Particle in a Backward-Facing Step Flow, *Int. J. Multiphase Flow*, 2001, vol. 27, pp. 1517–1532.
4. Zaichik, L.I., Kozelev, M.V., and Pershukov, V.A., Prediction of Turbulent Gas-Dispersed Channel Flow with Recirculation Zones, *Fluid Dyn.*, 1994, vol. 29 pp. 65–75.
5. Chan, C.K., Zhang, H.Q., and Lau, K.S., Numerical Simulation of Gas-Particle Flows behind a Backward-Facing Step Using an Improved Stochastic Separated Flow Model, *J. Comput. Mech.*, 2001, vol. 27, pp. 412–417.
6. Mohanarangam, K. and Tu, J.Y., Two-Fluid Model for Particle-Turbulence Interaction in a Backward-Facing Step, *AIChE J.*, 2007, vol. 53, pp. 225–2264.
7. Benavides, A. and Van Vachem, B., Eulerian-Eulerian Prediction of Dilute Turbulent Gas-Particle Flow in a Backward-Facing Step, *Int. J. Heat Fluid Flow*, 2009, vol. 30, pp. 452–461.
8. Mukin, R.V. and Zaichik, L.I., Nonlinear Algebraic Reynolds Stress Model for Two-Phase Turbulent Flows Laden with Small Heavy Particles, *Int. J. Heat Fluid Flow*, 2012, vol. 33, pp. 81–91.



9. Riella, M., Kahraman, R., and Tabor, G.R., Reynolds-Averaged Two-Fluid Model Prediction of Moderately Dilute Fluid-Particle Flow over a Backward-Facing Step, *Int. J. Multiphase Flow*, 2018, vol. 106, pp. 95–108.
10. Hishida K., Nagayasu T., and Maeda M., Augmentation of Convective Heat Transfer by an Effective Utilization of Droplet Inertia *Int. J. Heat Mass Transfer*, 1995, vol. 38, pp. 1773–1785.
11. Miyafuji, Y., Senaha, I., Oyakawa, K., and Hiwada, M., Enhancement of Heat Transfer at Downstream of a Backward-Facing Step by Mist Flow, in *Proc. 2nd Int. Conf. on Jets, Wakes and Separated Flows ICJWSF-2008*, Berlin, 2008.
12. Pakhomov, M.A. and Terekhov, V.I., Comparison of the Eulerian and Lagrangian Approaches in Studying the Flow Pattern and Heat Transfer in a Separated Axisymmetric Turbulent Gas-Droplet Flow, *J. Appl. Mech. Techn. Phys.*, 2013, vol. 54, no. 4, pp. 596–607.
13. Lobanov, P., Pakhomov, M., and Terekhov, V., Experimental and Numerical Study of the Flow and Heat Transfer in a Bubbly Turbulent Flow in a Pipe with Sudden Expansion. *Energies*, 2019, vol. 12, p. 2735.
14. Pakhomov, M.A. and Terekhov, V.I., Droplet Evaporation in a Two-Phase Mist Dilute Turbulent Flow behind a Backward-Facing Step, *Water*, 2021, vol. 13, p. 1335823.
15. Balakhrisna, T., Ghosh, S., Das, G., and Das, P.K., Oil-Water Flows Through Sudden Contraction and Expansion in a Horizontal Pipe—Phase Distribution and Pressure Drop, *Int. J. Multiphase Flow*, 2010, vol. 36, pp. 13–24.
16. Zhang, D. and Goharzadeh, A., Effect of Sudden Expansion on Two-Phase Flow in a Horizontal Pipe, *Fluid Dyn.*, 2019, vol. 54, no. 1, pp. 123–136.
17. Celis, G.E.O., Rosero, C.M.P., Loureiro, J.B.R., and Silva Freire, A.P., Breakup and Coalescence of Large and Small Bubbles in Sudden Expansions and Contractions in Vertical Pipes, *Int. J. Multiphase Flow*, 2021, vol. 137, p. 103548.
18. Yua, K.F., Lau, K.S., and Chan, C.K., Numerical Simulation of Gas-Particle Flow in a Single-Side Backward-Facing Step Flow, *J. Comp. Appl. Math.*, 2004, vol. 163, pp. 319–331.
19. Wang, B., Zhang, H.Q., and Wang, X.L., Large Eddy Simulation of Particle Response to Turbulence along Its Trajectory in a Backward-Facing Step Turbulent Flow, *Int. J. Heat Mass Transfer*, 2006, vol. 49, pp. 415–420.
20. Zhou, L.X. and Liu, Y., Two-Fluid LES and RANS Modeling of Sudden-Expansion Gas-Particle Flows, *Powder Technol.*, 2018, vol. 323, pp. 4–50.
21. Wang, H., Zhao, H., Guo, Z., He, Y., and Zheng, C., Lattice Boltzmann Method for Simulations of Gas-Particle Flows over a Backward-Facing Step, *J. Comp. Phys.*, 2013, vol. 239, pp. 57–71.
22. Balachandar, S. and Eaton, J.K., Turbulent Dispersed Multiphase Flow *Ann. Rev. Fluid Mech.*, 2010, vol. 42, pp. 111–133.
23. Varaksin, A.Y., Collision of Particles and Droplets in Turbulent Two-Phase Flows, *High Temp.*, 2019, vol. 57, no. 4, pp. 555–572.
24. Pakhomov, M.A. and Terekhov, V.I., Second Moment Closure Modelling of Flow, Turbulence and Heat Transfer in Droplet-Laden Mist Flow in a Vertical Pipe with Sudden Expansion *Int. J. Heat Mass Transfer*, 2013, vol. 66, pp. 210–222.
25. Fadai-Ghotbi, A., Manceau, R., and Boree, J., Revisiting URANS Computations of the Backward-Facing Step Flow Using Second Moment Closures. Influence of the Numerics, *Flow, Turb. Combust.*, 2008, vol. 81, pp. 395–410.
26. Nigmatulin, R.I., *Dynamics of Multiphase Media*, vol. 1, CRC Press, 1990.
27. Elghobashi, S., On Predicting Particle-Laden Flows, *Appl. Sci. Res.*, 1994, vol. 52, pp. 309–329.
28. Osipov, A.N., Mathematical Modeling of Dusty-Gas Boundary Layers, *Appl. Mech. Rev.*, 1997, vol. 50, pp. 357–370.
29. Thangam, S. and Speziale, C.S., Turbulent Flow past a Backward-Facing Step: A Critical Evaluation of Two-Equation Models, *AIAA J.*, 1992, vol. 30, pp. 1314–1320.
30. Zajkov, L.A., Strelets, M.Kh., and Shur, M.L., Comparison between One- and Two-Equation Differential Turbulence Models in Application to Separated and Attached Flows. Flow in a Channel with a Backward Facing Step, *High Temp.*, 1996, vol. 34, no. 5, pp. 713–725.
31. Derevich, I.V., Statistical Modelling of Mass Transfer in Turbulent Two-Phase Dispersed Flows, 1. Model Development, *Int. J. Heat Mass Transfer*, 2000, vol. 43, pp. 3709–3723.
32. Kutateladze, S.S. and Leont'ev, A.I., *Heat and Mass Transfer in Turbulent Boundary Layer*, New York: Hemisphere, 1990.